

Diverse organic carbon dynamics captured by radiocarbon analysis of distinct compound classes in a grassland soil

Katherine E. Grant^{1*}, Marisa N. Repasch^{1,2,3}, Kari M. Finstad¹, Julia D. Kerr¹, Maxwell Marple¹, Christopher J. Larson^{1,4}, Taylor A. B. Broek¹, Jennifer Pett-Ridge^{1,5}, and Karis J. McFarlane¹

¹Physical and Life Sciences Directorate, Lawrence Livermore National Laboratory, Livermore, CA 94550, USA

²Institute of Arctic and Alpine Research, University of Colorado, Boulder, CO, USA

³Earth and Planetary Sciences, University of New Mexico, Albuquerque, NM, USA

⁴Department of Earth and Environmental Science, University of Pennsylvania, Philadelphia, PA, USA

⁵Life and Environmental Sciences Department, University of California-Merced, Merced, CA, USA

Correspondence to: Katherine E. Grant (grant39@llnl.gov)

Abstract. Soil organic carbon (SOC) is a large, dynamic reservoir composed of a complex mixture of plant and microbe derived compounds with a wide distribution of cycling timescales and mechanisms. The distinct residence times of individual carbon components within this reservoir depend on a combination of factors, including compound reactivity, mineral association, and climate conditions. To better constrain SOC dynamics, bulk radiocarbon measurements are commonly used to trace biosphere inputs into soils and estimate timescales of SOC cycling. However, understanding the mechanisms driving the persistence of organic compounds in bulk soil requires analyses of SOC pools that can be linked to plant sources and microbial transformation processes. Here, we adapt approaches, previously developed for marine sediments, to isolate organic compound classes from soils for radiocarbon (¹⁴C) analysis. We apply these methods to a soil profile from an annual grassland in Hopland, California (USA) to assess changes in SOC persistence with depth to 1 m. We measured the radiocarbon values of water extractable organic carbon (WEOC), total lipid extracts (TLE), total hydrolysable amino acids (AA), and an acid-insoluble (AI) fraction from bulk and physically separated size fractions (<2 mm, 2 mm–63 μm, and <63 μm). Our results show that Δ¹⁴C values of bulk soil, size fractions, and extracted compound classes became more depleted with depth, and individual SOC components have distinct age-depth distributions that suggest distinguishable cycling rates. We found that AA and TLE cycle faster than the bulk soils and the AI fraction. The AI was the most ¹⁴C depleted fraction, indicating it is the most chemically inert in this soil. Our approach enables the isolation and measurement of SOC fractions that separate functionally distinct SOC pools that can cycle relatively quickly (e.g., plant and microbial residues) from more passive or inert SOC pools (associated with minerals or petrogenic) from bulk soils and soil physical fractions. With the effort to move beyond SOC bulk analysis, we find that compound class ¹⁴C analysis can improve our understanding of SOC cycling and disentangle the physical and chemical factors driving OC cycling rates and persistence.

32 **1 Introduction**

33 Soil organic carbon (SOC) is a large and complex terrestrial reservoir of Earth's organic carbon (OC) (Jobbágy and
34 Jackson, 2000). It is a highly dynamic and open pool with inputs from decaying plant material, living roots, and soil microbes,
35 and with losses driven by microbial activity that includes the degradation and transformation of compounds (Angst et al.,
36 2021). The result of these processes is a heterogenous mixture of organic compounds with different radiocarbon (^{14}C) ages
37 and reactivities (Lehmann and Kleber, 2015; Shi et al., 2020; Trumbore and Harden, 1997; Gaudinski et al., 2000; McFarlane
38 et al., 2013). This complexity obscures the mechanisms that control overall OC persistence in soils, resulting in a continued
39 debate over the degree to which environmental factors, physical protection, and chemical composition influence SOC reactivity
40 and persistence (Lützow et al., 2006; Lehmann et al., 2020; Schmidt et al., 2011).

41 Bulk analysis methods do not satisfactorily demonstrate how physical protection and chemical composition interact to
42 influence SOC persistence, and so novel organic matter characterization methods can shed light on how different compound
43 classes of OC are preserved in soils and through what mechanisms. For example, we need to understand how the chemical
44 structure of OC influences interactions with mineral surfaces, such as aggregation or sorption, as well as how the environment
45 influences the decomposition and resource availability of certain OC compounds and functional groups (Lehmann and Kleber,
46 2015; Schmidt et al. 2011; Kleber et al., 2021). However, it has been difficult to isolate, identify, and quantify pools of OC
47 without altering OC molecular chemistry (Von Lutzow et al., 2007). Thus, specific organic compounds isolated from soils,
48 such as amino acids and lipids (Rethemeyer et al., 2004), can provide information on how OC is stabilized in different
49 environments. Therefore, multiple approaches, such as a physical separation followed by a chemical separation, are needed to
50 fully understand the interplay between chemical compound reactivity and how carbon-mineral interaction functions as part of
51 SOC persistence in soil.

52 One approach used to investigate the controls on SOC persistence is to separate soil into operationally defined carbon
53 pools (e.g., size or density fractions) and characterize the resulting fractions. This approach has demonstrated that association
54 of OC with soil minerals is a critical mechanism for C stabilization (Vogel et al., 2014; Mikutta et al., 2007), as ^{14}C data
55 indicate that some mineral-associated C can persist for thousands of years (Torn et al., 2009). However, ^{13}C labelling
56 experiments show that some mineral-associated C cycles quickly, within months to years (Keiluweit et al., 2015; De Troyer
57 et al., 2011). Some biomolecules form strong associations with mineral surfaces, such as long-chain lipids with iron oxides
58 (Grant et al., 2022), while other compounds only loosely associate with minerals such as through hydrophobic interactions
59 with other OC compounds (Kleber et al., 2007). Therefore, physically isolated mineral-associated OC is still a heterogenous
60 mixture of OC molecules that have a distribution of turnover times, rather than a single homogenous and intrinsically stable
61 SOC pool (Stoner et al., 2023; Van Der Voort et al., 2017).

62 Another approach that can yield finer resolution of OC turnover than traditional techniques is to isolate and measure the
63 isotopic signature of specific compounds (Von Lutzow et al., 2007). In marine, riverine, and lacustrine systems, compound

64 specific radiocarbon analysis (CSRA) has been used monitor the degradation of organic carbon through the marine water
65 column (Loh et al., 2004), characterize marine particulate OC (Hwang and Druffel, 2003), constrain terrestrial OC burial and
66 export from river systems (Galy et al., 2015; Galy et al., 2008; Repasch et al., 2021, Smittenberg et al., 2004), and determine
67 effect of OC export and burial on precipitation patterns and climate (Hein et al., 2020; Eglinton et al., 2021). Different types
68 of compounds including plant or microbial lipid biomarkers (Douglas et al., 2018; Huang et al., 1996), amino acids (Bour et
69 al., 2016; Blattmann et al., 2020), lignin (Feng et al., 2017; Feng et al., 2013), certain carbohydrate compounds (Kuzyakov et
70 al., 2014; Gleixner, 2013), and pyrogenic or black carbon (Coppola et al., 2018) can be isolated and analysed for ^{14}C leading
71 to a more detailed understanding of the cycling of targeted compounds in the environment.

72 Each of these specific compounds can provide information related to the persistence, source, and potential fate of OC in
73 soils. For instance, lipids are found in plant cell walls and microbial cell membranes and are used for energy storage. Amino
74 acids are necessary for protein formation, are enriched in nitrogen relative to other plant and microbial residues, and likely
75 play an important role in nitrogen mining and recycling. These two compound classes have diverse chemical reactivities which
76 allows for insight into chemical compound persistence. Understanding the abundance and age of these two biomarkers in soils
77 can help differentiate the source of C used by soil microbes for metabolism and growth (e.g., new C inputs vs older, recycled
78 soil C) as well as the transformation pathways that yield persistent SOC.

79 Recently, CSRA approaches developed for these environments have been applied to soil showing promise for identifying
80 distinct ages of plant and microbial biomarkers in SOC (Gies et al., 2021; Grant et al., 2022; Van Der Voort et al., 2017; Jia
81 et al., 2023; Douglas et al., 2018). Most of these CSRA studies applied to SOC have targeted specific, individual biomarkers
82 in soils, which generally contribute less than 5% of the entire carbon pool (Lützow et al., 2006; Kögel-Knabner, 2002). This
83 approach can be too specific to elucidate holistic mechanisms for SOC persistence and turnover that pertain to the majority of
84 SOC. While individual biomarker ages, such as single ages of a particular lipid or single amino acid, can be useful in some
85 contexts, comprehensive understanding of carbon compound class persistence is vital for understanding and modelling the
86 vulnerability of soil carbon to degradation.

87 To strike a balance between too specific and too broad, some researchers have characterized broader compound classes
88 rather than isolating a single biomarker. For example, this ^{14}C -compound class approach has been applied to marine dissolved
89 and particulate OC with a range of compounds, such as total lipids and total amino acids, to provide a broader understanding
90 of OC persistence in oceans (Wang et al., 2006; Wang et al., 1998; Wang and Druffel, 2001; Loh et al., 2004). Wang et al.
91 (1998) established a sequential extraction procedure to analyse ^{14}C abundance of total lipids, amino acids, carbohydrates, and
92 a residual acid insoluble fraction from marine POC and sediments. This approach yielded distinct differences in ^{14}C age and
93 abundance of the amino acids, lipids, and the acid insoluble fraction in POC from the marine water column and sediment, as
94 well as in coastal versus open ocean environments. Loh et al. (2004) found the lipid fraction of dissolved OC and POC to be
95 the oldest fraction measured in both the Atlantic and Pacific oceans, while the acid insoluble fraction was intermediate in age,

96 and the amino acids and carbohydrates contained a significant contribution of modern carbon. Wang and Druffel (2001) also
97 used this approach and found that the lipids were the oldest compound class from sediments in the Southern Ocean, but the
98 acid insoluble residue was very similar in age to the lipid fraction. These studies suggest that compound classes can have
99 independent cycling rates, but these cycling rates can be influenced by the environment.

100 Here, we apply a ^{14}C compound class approach to soils to more broadly understand SOC turnover mechanisms. We
101 characterize the distribution and ^{14}C age of multiple SOC pools with depth in a well-studied annual grassland in California,
102 using soil physical fractionation (McFarlane et al., 2013; Poeplau et al., 2018) and modified compound class extraction
103 methods previously detailed for marine sediments (Wang et al., 1998). We measured the radiocarbon values of water
104 extractable organic carbon (WEOC), total lipid extracts (TLE), total hydrolysable amino acids (AA), and an acid-insoluble
105 (AI) fraction from bulk and physically separated size fractions (bulk soil, sand, and silt+clay). We expected the TLE to be
106 older than its source fraction (bulk soil, sand, or silt+clay), to be older with depth as the decline in plant inputs necessitates
107 recycling and use of older SOC, and to be older in the silt+clay fraction as its high surface area should result in mineral-OC
108 associations that protect SOC from soil microbes (Grant et al., 2022; Van der vort et al., 2017). We expected the AA to be
109 younger than the TLE fraction and the bulk SOC pool based on the young ^{14}C ages found for AA extracted from in marine
110 sediments (Wang et al., 1998; Wang and Druffel, 2001), but hypothesized that recycling of amino acids at depth by soil
111 microbes might result in an increase in the age of AA below 50 cm. Finally, we expected AI to have old C, similar to the TLE,
112 as seen found in marine sediments (Wang et al., 1998). Here, we describe the relative abundance and radiocarbon content of
113 WEOC, total lipid, amino acid, and acid insoluble compound class extracts in bulk soils and compare carbon storage and
114 cycling rates within soil size fractions. These data provide a foundation for the continued application of compound class ^{14}C
115 work to the understanding and modelling of soil OC persistence.

116 **2 Materials and Methods**

117 **2.1 Site and Sample Description**

118 Soil samples were collected from the University of California's Hopland Research and Extension Center (HREC) in January
119 2022. The site is an annual grassland with a Mediterranean-type climate, where the mean annual precipitation (MAP) is 940
120 mm per year and mean annual temperature is 15°C (Nuccio et al., 2016). The underlying geology consists of mixed sedimentary
121 rock of the Franciscan formation. The soils are designated Typic Haploxeralfs of the Witherall-Squawrock complex (Soil
122 Survey Staff, 2020). The samples were collected from the "Buck" site (39.001° , -123.069°) where the vegetation is dominated
123 by annual wild oat grass, *Avena barbata* (Kotanen, 2004; Bartolome et al., 2007). Soils were collected from a freshly dug soil
124 pit at four depths: 0–10 cm, 10–20 cm, 20–50 cm, and 50–100 cm. The site is dominated by annual grasses, shallow rooted
125 herbs, and forbs, and we did not observe roots below 10 cm. Thus, root derived inputs of OC are important near the soil surface,
126 but do not directly affect deeper soils at this site. Samples were stored in sealed plastic bags at ambient temperature and

127 transported to the laboratory in Livermore, CA. Soil samples were air dried, homogenized, and sieved to 2 mm, with the >2
128 mm fraction retained for further analysis. Samples were subdivided for soil characterization, physical size separations,
129 chemical compound extractions, and density fractionation.

130 **2.2 Physical Fractionation**

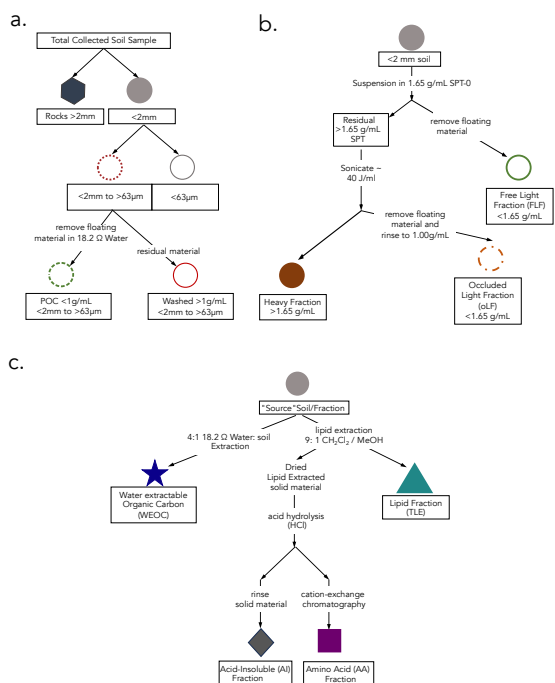
131 To compare compound classes between mineral-associated OC and mineral-free OC, we used a salt-free and chemical-free
132 method for isolating the mineral-associated organic matter from the free particulate organic matter (Fig. 1a). Under the
133 assumption that mineral-associated carbon is primarily found in the silt+clay (<63 μm) particle size fraction, we used a size
134 fractionation sieving method where air-dried samples were dry-sieved into three size fractions: bulk soil (<2 mm), sand (2 mm
135 - 63 μm), and silt+clay (<63 μm) (Lavalée et al., 2020; Poeplau et al., 2018). Additionally, because the majority of free
136 particulate organic carbon (POC) is contained in the sand fraction, we used a “water density” separation to remove the low
137 density POC from the mineral matter in this fraction, by suspending the sand fraction in 18.2 M Ω and removing the floating
138 OC, resulting in a POC (<1g mL⁻¹) fraction and a POC-free (>1g mL⁻¹) sand fraction.

139 To further characterize these soils and aid in interpretation of our data, we compared the size fractionated samples to samples
140 separated by density using sodium polytungstate (SPT-0 adjusted to a density of 1.65 g mL⁻¹) (Poeplau et al., 2018) (see SI
141 Section 1.1 for detailed methods). We chose to focus our compound class extraction efforts on size fractionated samples to
142 avoid chemical alteration of SOC during exposure to SPT, since SPT has a high ionic strength and low pH.

143 To constrain any contributions of OC from parent materials to SOC, we processed and analyzed the rock fraction (> 2mm)
144 (Agnelli et al., 2002; Trumbore and Zheng, 1996). Rocks were washed with 18.2 M Ω water in an ultrasonic bath to remove
145 surface contamination, rinsed with 1N HCl to remove any additional weathered material loosely adhered to the surface, dried
146 at 60°C, then manually crushed.

147 A large, representative aliquot (~10 g) of the bulk and each physical fraction were ball milled and measured for total organic
148 carbon (TOC, wt %), C/N ratio, $\delta^{13}\text{C}$ and $\Delta^{14}\text{C}$ (Section 2.6). In addition, we analyzed the bulk soils at each depth with nuclear
149 magnetic resonance (¹³C NMR) to assess the broad structural complexity of the OC in the bulk soil (SI Section 2).

150



151
 152 **Figure 1: Schematics of protocols used in this study for a) fractionation by size, b.) density separation (details in SI methods), and**
 153 **c) extraction of targeted compound classes. The “source soil/fraction” refers to the soil from which the different compound classes**
 154 **are extracted. All compound extractions and physical fractionations were applied to the <2 mm bulk soil; total lipid extract (TLE),**
 155 **amino acid (AA), and acid insoluble (AI) compound classes were also extracted from the silt+clay fraction; and only the TLE was**
 156 **extracted from the dense fraction (DF).**

157
 158 **2.3 Water-extractable organic carbon (WEOC)**

159 The water-extractable organic carbon (WEOC) fraction was collected from 80 g of bulk soil with 18.2 MΩ water using a 4:1
 160 water to soil ratio (Van Der Voort et al., 2019; Lechleitner et al., 2016; Hagedorn et al., 2004). Saturated soil samples were
 161 shaken for 1 hour and then filtered through a pre-rinsed 0.45 µm polyethersulfone (PES) Supor filter under vacuum. An aliquot
 162 was taken for dissolved organic carbon (DOC) measurement on a Shimadzu TOC-L combustion catalytic oxidation instrument.
 163 Sample concentrations were determined using a nine-point DOC calibration curve ranging from 0–200 mgC L⁻¹. The WEOC
 164 fraction was dried using a Labconco CentriVap centrifugal drying system at 40°C and subsequently transferred with 0.1N HCl
 165 into pre-combusted quartz tubes to eliminate any inorganic carbon dissolved in the aqueous fraction. The acidified WEOC
 166 fractions were then dried down using the CentriVap. Dried samples were flame sealed under vacuum (Section 2.6) for
 167 subsequent carbon isotope analyses.

169 **2.4 Total Lipid Extraction (TLE)**

170 Total lipids (TLE) were extracted from the soil samples using an Accelerated Solvent Extraction (ASE) system (Dionex 350,
171 Thermo Scientific) in duplicate. The TLE was extracted from the bulk, sand, silt+clay, and the dense fraction ($> 1.65 \text{ g ml}^{-1}$;
172 DF). An aliquot of 10–30 g of soil was loaded into a stainless-steel ASE extraction cell depending on TOC content (Rethemeyer
173 et al., 2004). The ASE was set to extract the sample for 5 minutes with a holding temperature of 100°C at 1500 PSI. Lipids
174 were extracted using a 9:1 ratio of dichloromethane (DCM or syn: methylene chloride) to methanol (Wang et al., 1998; Van
175 Der Voort et al., 2017; Grant et al., 2022). The TLE was dried under constant ultra-pure N_2 flow at 40°C using a nitrogen dryer
176 (Organomation Multivap Nitrogen Evaporator). The TLE was resuspended in $\sim 5\text{ml}$ of 9:1 DCM:Methanol then transferred to
177 pre-combusted quartz tubes, dried again, and analyzed for ^{14}C as described below (Section 2.5). Total CO_2 produced by the
178 combustion of the TLE was measured manometrically on the ^{14}C vacuum lines during graphitization. Process blank samples
179 were analyzed with each batch (SI Section 3.1).

180

181 **2.5 Amino Acid (AA) Extraction**

182 Amino acids (AA) were extracted from the lipid-extracted residual bulk and silt+clay size fraction with an acid hydrolysis
183 procedure, desalted, and isolated with cation exchange chromatography using methods modified from those used in marine
184 systems (Wang et al., 1998; Ishikawa et al., 2018; Blattmann et al., 2020). Briefly, a 500 mg soil aliquot was hydrolyzed with
185 6N HCl (ACS grade) under an N_2 atmosphere for 19-24 hours at 110°C . After hydrolysis, amino acids in solution were
186 separated from the solid acid insoluble (AI) fraction via centrifugation for 5 minutes at 2500 rpm. The AI fraction was
187 subsequently washed at a minimum three additional times with 0.2N HCl to ensure complete AA recovery. The supernatant
188 was collected in a single pre-combusted vial and then filtered through a pre-combusted quartz wool fiber plug to remove
189 extraneous sediment particles. The filtered hydrolysate was dried using a CentriVap at 60°C for 4 hours. The dried supernatant
190 was redissolved in 1 ml 0.1N HCl and loaded onto a preconditioned resin column (BioRad 50WX8 200-400 mesh resin) to
191 isolate the AA from other hydrolyzed organic matter and remove excess chloride. Details of the procedure can be found in
192 Ishikawa et al., 2018. Briefly, once the sample was loaded on the column, it was rinsed with three bed volumes ($\sim 6 \text{ ml}$) of 18.2
193 $\text{M}\Omega \text{ H}_2\text{O}$. The free AA were eluted with 10 ml of 2N ammonium hydroxide (NH_4OH), then transferred into pre-baked quartz
194 tubes, dried at 60°C in the CentriVap, and finally sealed and combusted for isotopic analysis. The remaining rinsed solid
195 residual after hydrolysis is the acid-insoluble (AI) fraction. These are processes as a solid sample for isotopic analysis.

196

197 **2.6 Isotopic and elemental analysis**

198 All samples were analyzed for radiocarbon (^{14}C) at the Center for Accelerator Mass Spectrometry (CAMS) at Lawrence
199 Livermore National Lab (LLNL) in Livermore, California. Samples were either measured on a 10 MV Van de Graaf FN or
200 1MV NEC Compact accelerator mass spectrometer (AMS) (Broek et al., 2021), with average errors of $F^{14}\text{C} = 0.0035$. For

201 solid soil analysis, 10 to 250 mg of ground material was weighed into a pre-combusted quartz tubes along with 200 mg CuO
202 and Ag, flame sealed under vacuum, then combusted at 900°C for 5 hours. The CO₂ was reduced to graphite on preconditioned
203 iron powder under H₂ at 570°C (Vogel et al., 1984). Measured ¹⁴C values were corrected using δ¹³C values and are reported
204 as age-corrected Δ¹⁴C values using the following the conventions of Stuiver and Polach (1977). Extraneous C was quantified
205 for the TLE and AA extractions (SI Table 4 and SI Section 3). For ease of reference, we included conventional radiocarbon
206 ages in our figures and tables. We quantified turnover times using the single pool turnover model described in Sierra et al.
207 (2014) and Van Der Voort et al. (2019) and explained in detail in Trumbore (2000) and Torn et al. (2009). This approach
208 generates two solutions for pools with Δ¹⁴C > 0 ‰, one corresponding to each side of the atmospheric ¹⁴C-CO₂ curve over the
209 last 70 years (Hua et al., 2022). Unfortunately, we cannot identify the correct solution (McFarlane et al., 2013; Trumbore,
210 2000), especially for TLE and AA fractions from the top 20 cm, as we do not have multiple time points or additional constraints
211 such as pool-specific input or decomposition rates (see Section 2.8). Therefore, our data analysis and interpretations rely on
212 the reported Δ¹⁴C values. All individual ¹⁴C measurements used in this study are listed in the Supplementary Information (SI
213 Table 1 and 2).

214 For each solid sample, a dried homogenized aliquot was analyzed for TOC concentration and δ¹³C using an elemental analyzer
215 (CHNOS) coupled to an IsoPrime 100 isotope ratio mass spectrometer at the Center for Stable Isotope Biogeochemistry (CSIB)
216 at the University of California, Berkeley. Samples are assumed to have no inorganic carbon based on acid leaching tests and
217 previously published ¹⁴C work at this site (Finstad et al, 2023, Foley et al., 2023). δ¹³C was measured in duplicate for each
218 solid sample and errors represent the standard deviation of the mean. δ¹³C values of WEOC, TLE, and AA extracts were
219 measured on a split of the cryogenically purified CO₂ and were analyzed at the Stable Isotope Geosciences Facility at Texas
220 A&M University on a Thermo Scientific MAT 253 Dual Inlet Stable Isotope Ratio Mass Spectrometer (SI Table 1).

221

222 **2.7 Data analysis**

223 Data was analyzed using MATLAB version R20223 and R v. 3.614 (R Core Team, 2019). Linear regressions were calculated
224 between the sample depth mid-point and Δ¹⁴C values from both the size fractions as well as the extracted compounds (WEOC,
225 TLE, AA, AI) from the different size fractions. This was done to directly compare the difference in Δ¹⁴C value between the
226 compound classes. Correlation coefficients, p-values and r² are provided in SI Table 3. Analysis of Variance (ANOVA) was
227 used to assess differences in Δ¹⁴C with depth, between TLE and AA, and between soil fractions. ANOVA tests were performed
228 in R v. 3.614 (R Core Team, 2019). In the text, results are reported as means followed by one standard error when n = 2 or 3
229 or by analytical error when n = 1.

230

231 **2.8 Interpretation of radiocarbon data**

232 In the interpretation of soil ^{14}C activity, we must consider how ^{14}C created during atmospheric nuclear weapons may have
233 affected the isotopic signatures of SOC at our study site. Significantly elevated “bomb” derived ^{14}C was released into the
234 environment during atmospheric nuclear weapons testing during the mid-20th century. This atmospheric radiocarbon spike has
235 been continuously incorporated into carbon reservoirs including vegetation, soils, and oceans (Levin and Hessshaimer, 2000).
236 Plants assimilate CO_2 with the ^{14}C signature of the current year’s atmosphere during photosynthesis and thus incorporate the
237 current atmospheric ^{14}C signature into their tissues and root exudates. This signature then cycles into and through soils as this
238 plant-derived organic matter decays, is processed by microbes, and enters stable soil organic matter pools (Torn et al. 2009).
239 Since the termination of atmospheric weapons testing in the 1960s and with continued fossil fuel emissions, the ^{14}C of
240 atmospheric CO_2 has decreased to approximately pre-1950 values with $0 \pm 1\text{‰}$ reported for the 2019 Northern Hemisphere
241 growing season (Hua et al. 2022). Thus, soil carbon pools with ^{14}C signatures above 0‰ can be interpreted as decadal-aged or
242 decadal cycling C and pools with ^{14}C signatures below 0‰ cycle on century to millennial timescales.

243

244 **3 Results**

245 **3.1 Radiocarbon values and characterization of the physical fractions**

246 We used soil size and density fractionation to separate the bulk soil into fractions with different degrees of mineral protection.
247 Radiocarbon content for the bulk soil, sand, and silt+clay (SI Table S3) became more ^{14}C depleted (older) with increasing
248 depth (Table 1, Fig. 2). SOC in the silt+clay was consistently younger than in the bulk soil, with the average difference in $\Delta^{14}\text{C}$
249 values increasing from 4‰ at the surface to 87‰ at depth. In the sand fraction, the $\Delta^{14}\text{C}$ values of POC were consistently near
250 current atmospheric values ($2 \pm 3\text{‰}$) and were not significantly correlated with depth. In contrast, the $\Delta^{14}\text{C}$ values of the POC-
251 free sand-sized fraction declined with depth ($25 \pm 3\text{‰}$ to $-510 \pm 2\text{‰}$, $p = 0.006$) and were indistinguishable from the POC-
252 free sand fraction (Fig. 2). Density fractionation of the bulk soil resulted in most of the sample mass ($> 98\%$) and OC (75–
253 83%) recovered in the DF at all depths (SI Fig. S2).

254

255

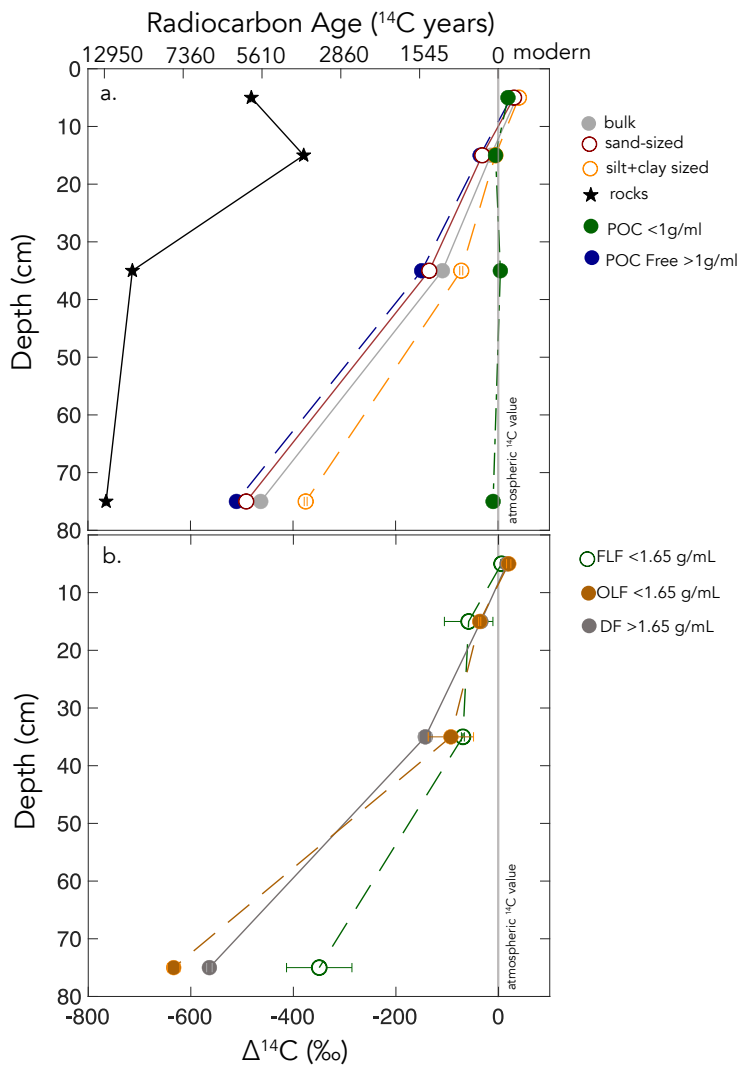
Table 1. Carbon concentrations, mass fractions, and radiocarbon values for the size separations from the Buck Pit

Depth	bulk (<2mm)				sand-sized (2mm to 63 μ m)				POC-free >1g mL ⁻¹				silt+clay (<63 μ m)			
	%OC	$\Delta^{14}\text{C} \pm$ err (‰)	<i>mass f</i>	%OC	$\Delta^{14}\text{C} \pm$ err (‰)	%OC	$\Delta^{14}\text{C} \pm$ err (‰)	%OC	$\Delta^{14}\text{C} \pm$ err (‰)	%OC	$\Delta^{14}\text{C} \pm$ err (‰)	<i>mass f</i>	%OC	$\Delta^{14}\text{C} \pm$ err (‰)	%OC	$\Delta^{14}\text{C} \pm$ err (‰)
0-10 cm	3.14	31 \pm 3	0.71	2.68	25 \pm 3	2.08	25 \pm 3	25.69	19 \pm 3	0.29	4.25	34 \pm 3				
10-20 cm	1.22	-22 \pm 3	0.69	0.94	-38 \pm 3	0.77	-35 \pm 3	25.99	-5 \pm 3	0.31	1.84	-13 \pm 3				
20-50 cm	0.50	-116 \pm 3	0.75	0.39	-142 \pm 3	0.38	-149 \pm 2	n.m.	4 \pm 3	0.25	0.85	-79 \pm 3				
50-100 cm	0.25	-468 \pm 3	0.79	0.23	-496 \pm 3	0.18	-510 \pm 2	n.m.	-10 \pm 3	0.21	0.35	-380 \pm 3				

256

257

258



259

260

261

262

263

264

265

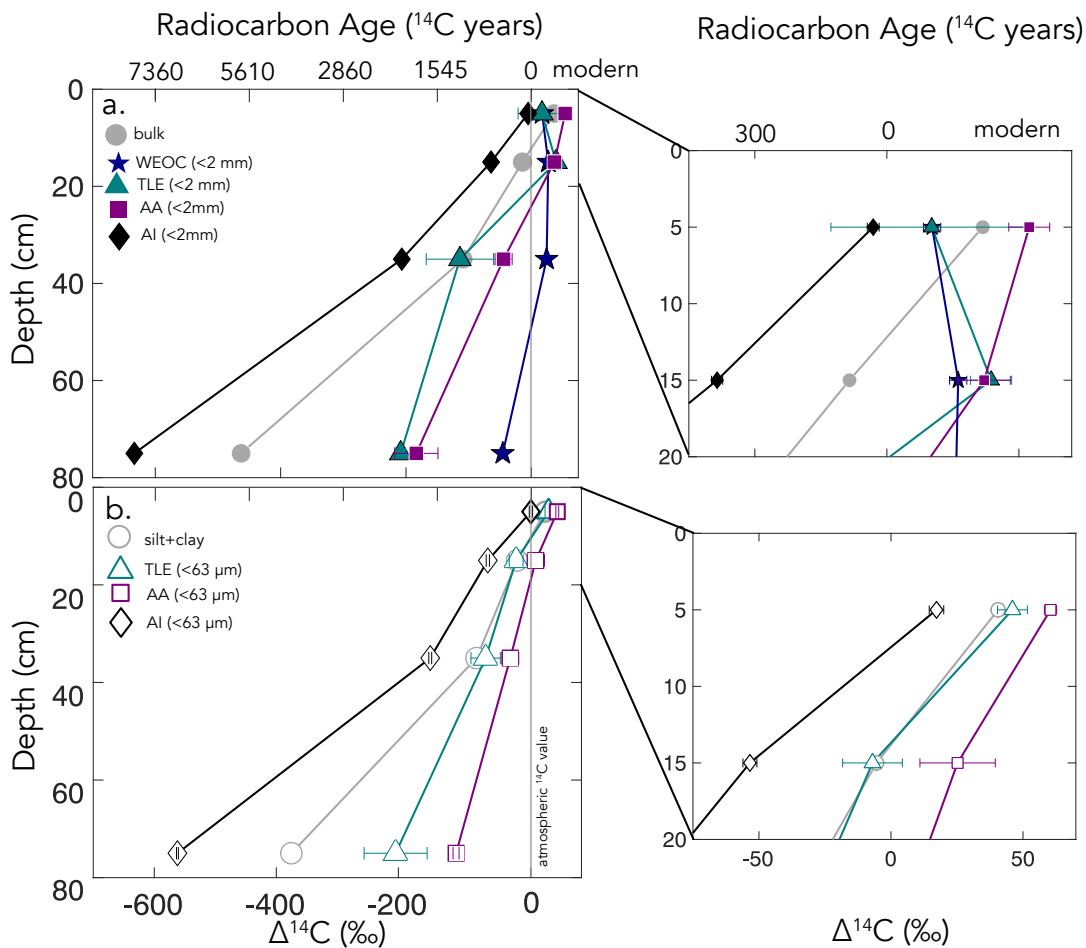
Figure 2: $\Delta^{14}\text{C}$ values by depth for a) size-fractions. b) density-fractions from the Buck soil pit. Conventional ^{14}C ages are provided for reference. The following abbreviations appear in the legend: particulate organic carbon (POC), free light fraction (FLF), occluded light fraction (OLF), and dense fraction (DF).

3.2 Compound Class results from bulk soil and silt+clay

266 In both the bulk soil and silt+clay fraction, the extracted compound classes became ^{14}C -depleted with depth except for the
267 WEOC, which had ^{14}C values that reflected C inputs recently fixed from the atmosphere throughout the soil profile (Fig. 2; SI
268 tables). The $\Delta^{14}\text{C}$ values of the WEOC ranged from $14 \pm 4\text{‰}$ at the surface to $-46 \pm 4\text{‰}$ at depth, and the DOC concentrations
269 ranged from 43.2 to $6.7 \text{ mg C g soil}^{-1}$ at the surface and at depth, respectively.

270 The TLE from the bulk soil had $\Delta^{14}\text{C}$ values that range from 17 ± 27 to $-208 \pm 6\text{‰}$ ($n = 2$; \pm SE) in the surface and
271 deepest sample, respectively. In comparison, the TLE from the silt+clay fraction was modern at the surface and became more
272 ^{14}C depleted with depth ($p < 0.001$), from 46 ± 4 to $-204 \pm 36 \text{‰}$. The slopes of the linear regressions of $\Delta^{14}\text{C}$ with depth were
273 indistinguishable in TLE from the bulk soil and silt+clay. In addition, the TLE from the bulk TLE and silt+clay fraction TLE
274 (SI Tables) had very similar $\Delta^{14}\text{C}$ values, but the bulk soil had less lipid-C extracted during each experiment ($280 \text{ } \mu\text{g g C}^{-1}$ in
275 the 0–10 cm vs. $150 \text{ } \mu\text{g g C}^{-1}$; SI Table 2).

276 The $\Delta^{14}\text{C}$ values of the AA extracted from the bulk soil ranged from 54 ± 5 to -183 ± 24 ($n = 2$, SE) with depth (Fig.
277 3, SI Table S3). Similarly, the $\Delta^{14}\text{C}$ value of the AA fraction extracted from silt+clay declined with depth from $60 \pm 3\text{‰}$ ($n =$
278 2 , SE) at the surface to $-106 \pm 4 \text{‰}$ ($n = 2$, SE) at 50–100 cm depth. The slopes of the AA extracted from the bulk and silt+clay-
279 size fractions were statistically different, indicating that the AA extracted from the bulk soil became more depleted with depth
280 than that extracted from the silt+clay (SI Table S3). Furthermore, AA fractions were enriched in ^{14}C relative to the TLE or AI
281 fraction ($p < 0.01$ for bulk soil and $p < 0.05$ for silt+clay). The AI fraction was the oldest fraction found in our study at each
282 depth. The $\Delta^{14}\text{C}$ values of the AI fraction ranged from $-5 \pm 2\text{‰}$ to $-633 \pm 2\text{‰}$ (analytical error, $n=1$) and declined with depth
283 ($p < 0.01$) for bulk soil and silt+clay (Fig. 3; SI Table S3).



284

285 **Figure 3: a) $\Delta^{14}\text{C}$ by depth for bulk soil and four compound class fractions extracted from bulk soil for the entire depth profile with**
 286 **the inset of the top 20 cm. b) $\Delta^{14}\text{C}$ by depth for the silt+clay (<63 μm) fraction and three compound classes extracted from the**
 287 **silt+clay for the entire depth profile with the inset of the top 20 cm. For total lipid extract (TLE) and amino acid (AA) fractions**
 288 **($n=2$) and error bars represent the standard error from duplicate measurements. For the <2 mm, water extractable organic carbon**
 289 **(WEOC), and acid insoluble (AI) fractions ($n=1$) and error bars represent analytical error. Error bars are smaller than the marker**
 290 **width where not shown.**

291

292

293 4 Discussion

294 4.1 Variability of ^{14}C in compound classes in soils

295 We measured radiocarbon content of four distinct soil chemical extracts: water extractable organic carbon (WEOC), total
 296 lipid extract (TLE), free amino acids (AA), and the acid insoluble fraction (AI), each of which had distinct $\Delta^{14}\text{C}$ values
 297 compared to the source soil it was extracted from (bulk or silt+clay; Fig. 4a and 4b). The central questions of this study are:

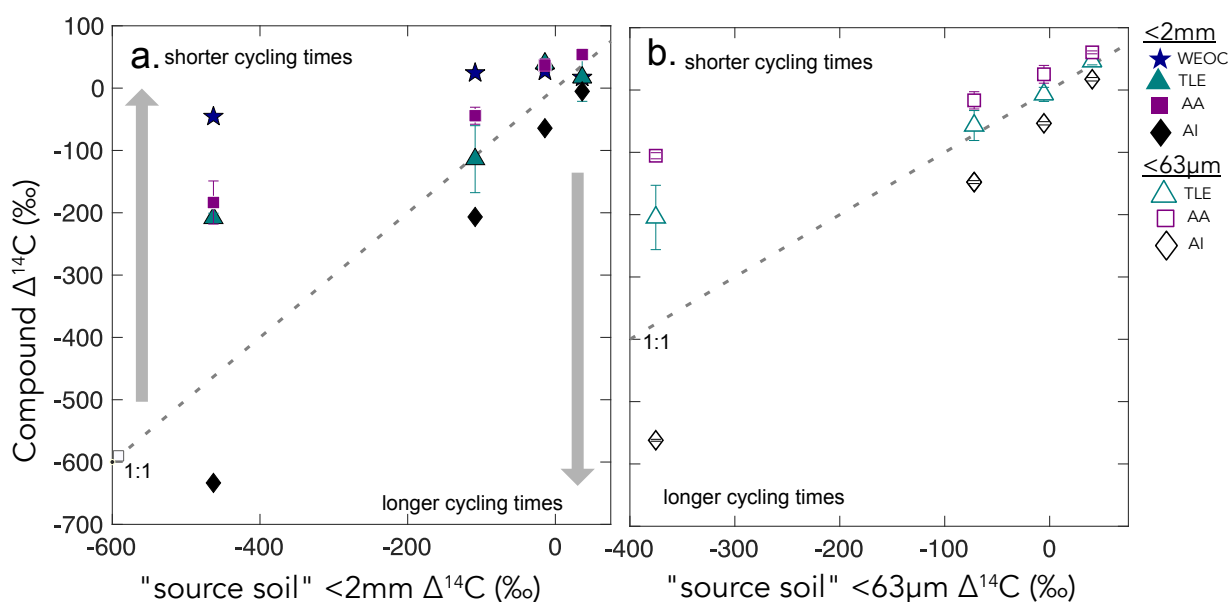
298 What are the differences in cycling time/age between various organic compounds in the soil? Do these differences in cycling
299 time change with depth? As expected, $\Delta^{14}\text{C}$ values of TLE, AA, and AI became more depleted with depth (Fig. 2). More
300 interestingly, the differences between the ^{14}C content of source soil and the extracted compounds were not consistent with
301 depth (Fig. 3a and 3b). This divergence in $\Delta^{14}\text{C}$ values reflects differences in turnover times among compound classes, which
302 can be influenced by the sources of OC to each of these pools and by differences in the stabilization mechanisms protecting
303 those compounds from decay. In this annual grassland, plant inputs should have a greater influence on SOC pools near the
304 surface, which we confirmed with near modern $\Delta^{14}\text{C}$ signatures in the 0–10 cm depth for all compound classes and size
305 fractions (Fig. 3b and 3c). Furthermore, at deeper depths, new vegetation inputs should be less readily available, which results
306 in more depleted $\Delta^{14}\text{C}$ signatures at depth and could necessitate microbial use and recycling of older SOC.

307 We found that, averaged across depths, the $\Delta^{14}\text{C}$ values of the TLE were more depleted than those of the AA, though both
308 compound classes were more enriched in $\Delta^{14}\text{C}$ than the bulk soil or silt+clay from which they were extracted. The extracted
309 AAs are the foundational units of hydrolysed proteins and found in both plant and microbial biomass (Blattmann et al., 2020).
310 As in marine studies, we found the AAs to be the youngest compound class fraction (of the TLE and AI) in these soils. The
311 AA pool likely reflects a more actively cycling microbial pool especially at depth, as AA are enriched in nitrogen compounds
312 and likely microbes are both preferentially mining and recycling these compounds (Moe, 2013). The divergence from bulk ^{14}C
313 values indicate that even at depth in the soil, the AAs are either continuously replenished from transport of AAs from surface
314 horizons or re-synthesized with relatively ^{14}C enriched sources such as the WEOC.

315 Based on published data for both soils and marine sediments, we expected the TLE to be older than both the AAs and the
316 bulk soil, however we found that all TLE samples, no matter what fraction we measured, were more ^{14}C enriched than the bulk
317 soil. TLE is composed of a continuum of lipids from plant and microbial materials, ranging from leaf waxes to microbial cell
318 structural components (Angst et al., 2021; Angst et al., 2016), that cycle at different rates and likely interact with mineral
319 surfaces. Previous studies where individual lipid biomarker $\Delta^{14}\text{C}$ values were measured in soils on either short chain or long
320 chain fatty acids found a divergence in $\Delta^{14}\text{C}$ values between these two pools, with short chain lipids generally having enriched
321 ^{14}C values and long chain lipids having more depleted ^{14}C values (Grant et al., 2022; Van Der Voort et al., 2017). For example,
322 long-chain lipid biomarkers, primarily thought to be plant derived, had consistently older ^{14}C ages than bulk soil (Van Der
323 Voort et al., 2017). Short-chain lipids, which can be microbial or root derived (Rethemeyer et al., 2004), were found to be
324 younger than long-chain lipids throughout the soil profiles and younger than bulk soil at depth (Van Der Voort et al., 2017).
325 However, microbial cell wall lipid biomarkers (glycerol dialkyl glycerol tetraethers, GDGTs) had older ^{14}C ages than bulk
326 soils (Gies et al., 2021). With this consideration, our result of more enriched ^{14}C of the TLE could be an indication of a
327 predominance of short chain lipids and suggested higher abundance of microbially-derived lipids than plant-derived lipids.
328 However further study of specific lipid abundance (e.g., *n*-alkanes, fatty acids) in these soils are necessary, as it is unclear to
329 what degree lipids are older than bulk soils with depth because of preservation of these compounds through mineral association

330 or because of microbial use of aged OC sources for growth.

331 We found that AI, the residual sample after both the TLE and AA have been extracted (Wang et al., 1998; Wang et al.,
332 2006). was the most ^{14}C depleted OC fraction measured at each soil depth (Fig. 3, 4) The AI fraction was far more depleted
333 relative to the bulk soil (Fig. 3a and 4a) than observed in marine studies with acid-insoluble OC (Wang et al., 2006; Wang and
334 Druffel, 2001). In these marine studies, the ^{14}C of the AI varied in age depending on sampling depth and location. The
335 significant depletion of the AI in our soils suggests that these chemically stable compounds are not oxidized in soil.
336 Importantly, our AI samples are older than the other chemical and physical soil fractions that we measured in the soil, consistent
337 with the general expectation that aromatic compounds can be difficult to degrade in in soils (Ukalska-Jaruga et al., 2019).
338



339

340 **Figure 4.** $\Delta^{14}\text{C}$ values of the three extracted compound classes, the water extractable organic carbon (WEOC), the total lipid extract
341 (TLE), the amino acid (AA) fraction, and the acid insoluble (AI) fraction, (y-axis) compared to the $\Delta^{14}\text{C}$ values of the source
342 soil/fraction (x-axis) for a) bulk soil and b) silt+clay. The grey dashed lines show the 1:1 line where bulk sample $\Delta^{14}\text{C}$ equals
343 compound class $\Delta^{14}\text{C}$. Gray arrows point to regions where data plot above or below the 1:1 line, suggesting that a given compound
344 class has shorter and longer carbon turnover times than bulk soil, respectively.
345

346 4.2 Differential OC cycling between fractionation methods

347 Our results suggest different OC cycling timescales for the different physical fractions representing the “source” fractions.
348 Here, we focus on the silt+clay fraction as an operationally defined mineral-associated OC pool. Numerous soil physical
349 fractionation schemes have been applied to soils and disparities in methods challenge interpretation and intercomparison of

350 results from different studies using different approaches. We compared the size-based soil fractionation to the density
351 fractionation to aid in interpretation and comparability of our findings to other studies. Our silt+clay fraction had higher $\Delta^{14}\text{C}$
352 values than the sand, POC-free sand, and the dense fraction (DF). Our silt+clay fraction could include free organic matter that
353 passed through the 63 μm sieve but that would have floated off the DF during density fractionation. For reference, the free
354 light fraction (FLF) has higher $\Delta^{14}\text{C}$ values than the mineral-associated pools and bulk soils (Fig. 5), but also has high C:N
355 reflecting the high OC content and dominantly plant origin of this fraction (SI Table S1). We assume that this small-size free
356 OC is a small fraction of the total silt+clay OC as no small fragments of organic matter were visible and because the C:N ratios
357 of the silt+clay fractions are only slightly elevated compared to the bulk soil and sand fractions (SI Table S1). Rather, the
358 silt+clay fractions may have higher $\Delta^{14}\text{C}$ values relative to the POC-free sand and bulk soil because higher surface area in the
359 silt+clay may facilitate mineral association with surface derived OC (e.g., from the WEOC fraction).

360 Additionally, our TLE comparison between different size and density fractions highlights the important influence that
361 method selection has over experimental results. Across studies, the mineral-associated OC is not a uniformly defined pool,
362 and the observed results are a consequence of the methodology used to separate the samples (Fig. 6). The mineral-associated
363 TLE cycled more rapidly than the bulk soil no matter which “mineral-associated” fraction (the silt+clay or the dense fraction)
364 was chosen (Fig. 6). The $\Delta^{14}\text{C}$ values of TLE from the bulk, sand, and silt+clay fractions were indistinguishable from one
365 another, possibly because the size fractionation scheme did not effectively separate distinct lipid pools. However, the $\Delta^{14}\text{C}$
366 values of TLE from the DF were significantly more ^{14}C depleted than TLE from the silt+clay size fraction (Fig. 6), suggesting
367 there were older lipids in the DF relative to the silt+clay. However, more depleted ^{14}C values found in the TLE from the DF
368 compared to the silt+clay could have resulted from the DF being exposed to SPT and/or ground after drying and before lipid
369 extraction. It is possible that grinding the DF prior to lipid extraction increased the exposed surface area and resulted in a larger
370 fraction of old SOC or rock-derived OC being incorporated into the TLE than if the DF had not been ground. We hesitate to
371 definitively choose a best method for fractionation because each soil environment and experiment require careful
372 methodological consideration and selection. However, given the clear differences in results between MAOM derived from
373 size and density fractionation, it appears grinding the samples prior to extraction had significant effects on the age of the
374 resulting TLE. Clearly, the approach used to fractionate soils influences experimental results and must be considered when
375 interpreting differences in persistence across operationally defined OC pools.

376

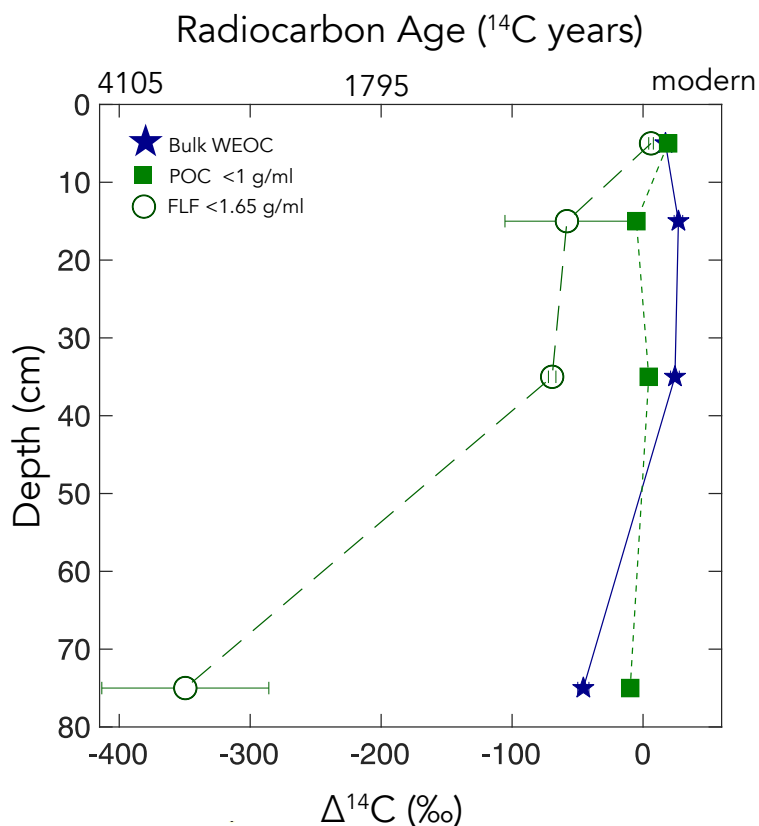
377 **4.3 Variation in OC cycling throughout the depth profile**

378 The WEOC (extracted from bulk soils) and POC ($<1\text{g mL}^{-1}$ floated off the sand-size fraction) had the highest $\Delta^{14}\text{C}$ values
379 throughout the soil profile, reflecting a predominance of modern carbon from plant detritus and root exudates to these pools.
380 WEOC fractions can comprise a complex mixture of molecules with different structures (Hagedorn et al., 2004; Bahureksa et
381 al., 2021), which are common only in their ability to be mobilized and dissolved in water. WEOC can mobilize and percolate

382 down the soil profile with sufficient precipitation to allow vertical transport. Both the POC and WEOC fractions supply OC
383 that is readily accessible for microbial degradation and microbial utilization – resulting in the rapid turnover and relatively
384 high $\Delta^{14}\text{C}$ values of these two pools (Marin-Spiotta et al., 2011). Occurrence of young OC in deep soils may be driven by
385 microbial uptake of this young and bioavailable DOC or POC. Additionally, we found that the free light-density fractions were
386 depleted in ^{14}C relative to the WEOC and POC (Fig. 5). We suspect this is due to colloidal particles in the FLF, which are not
387 dispersed or dense enough to settle in the SPT.

388 The study site has a Mediterranean climate, and these soils undergo seasonal wetting and drying cycles that may intensify
389 in the future (Swain et al., 2018), potentially shifting the composition or amount of OC that percolates down the soil column,
390 which could shift the age of the OC that the microbial community accesses at depth. Deeper in the soil profile, greater reactive
391 mineral surface area and lower microbial activity can enhance carbon stabilization in subsoils (Homyak et al., 2018; Dwivedi
392 et al., 2017; Pries et al., 2023). Further research is needed to understand the effects of seasonal wetting and drying on the
393 behaviour of water-soluble OC in the soil profile.

394 In general, the $\Delta^{14}\text{C}$ values of the TLE, AA, and AI fractions decreased with increasing depth in the profile. While all
395 extracted compounds followed this trend, the degree of ^{14}C depletion with depth varied somewhat between the different
396 compound classes and between the bulk and silt+clay source fractions. The TLE extracted from the bulk and from the silt+clay
397 fraction had similar slopes with depth. This suggests that depth has more influence than fraction size on resulting lipid ^{14}C
398 content, possibly because of limited transport of lipids down the soil profile. The AAs extracted from the bulk and from the
399 silt+clay fraction differed from one another in that the AA extracted from the bulk soil became more depleted with depth than
400 the AA extracted from the silt+clay. This suggests that at depth, AAs from the silt+clay fraction cycle more quickly than AA's
401 extracted from the bulk soil, possibly indicating that the silt+clay fraction is more directly influenced by microbial activity
402 than the sand fraction. At depths greater than 30 cm, the TLE and AA fraction were markedly younger than the bulk soil,
403 possibly resulting from transport of lipids and amino acids from surface horizons down profile, rapid recycling of these
404 compounds at depth, the use of a relatively modern C source for lipid and amino acid synthesis at depth, or most likely, a
405 combination of these. At all depths the AI was significantly older than the source fraction, indicating that throughout the soil
406 profile the AI contains an old and stable pool of OC.



407
 408 **Figure 5: Particulate organic carbon (POC) (floated from the sand, n = 1), free light fraction (FLF) (from bulk soil, n = 3, and error**
 409 **bars indicate standard error on the mean), and water extractable organic carbon (WEOC) (from bulk soil, n=1). $\Delta^{14}\text{C}$ values by**
 410 **depth. For POC and WEOC, error bars indicate analytical error are generally smaller than the symbols.**
 411

412 4.4 Compound class $\Delta^{14}\text{C}$ values in mineral-associated SOC

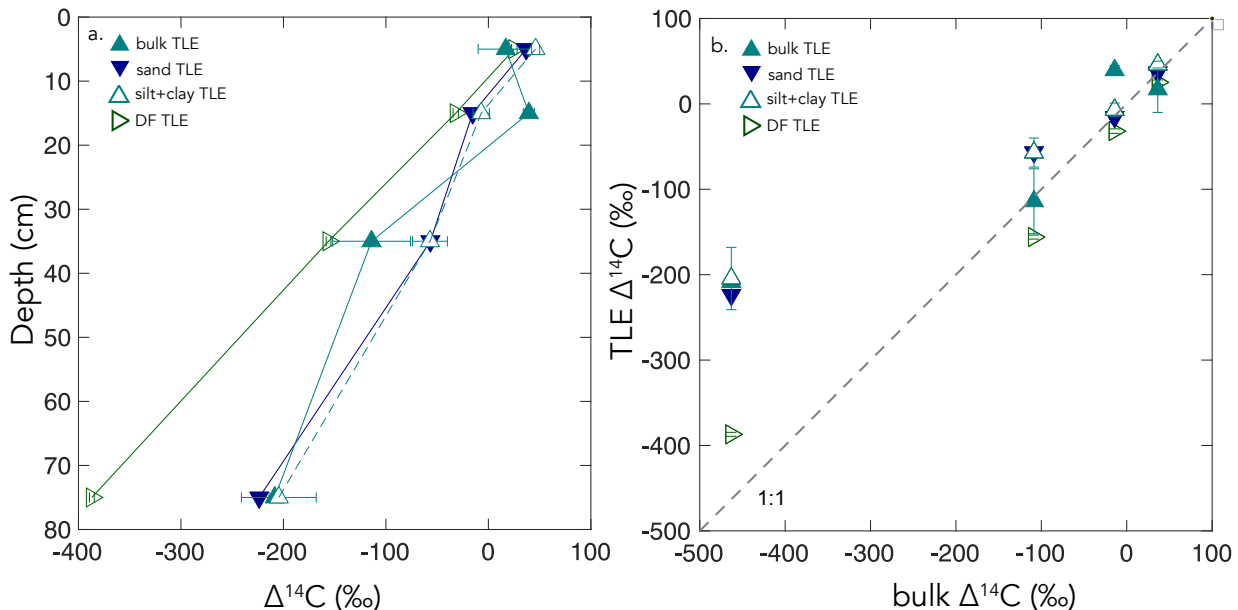
413 To investigate the effect of mineral interaction on the $\Delta^{14}\text{C}$ values or persistence of the TLE, AA, and AI, we measured
 414 these extracted compound classes from physical fractions intended to yield approximate mineral-associated carbon pools. We
 415 focused primarily on the silt+clay size fraction as the physical fraction that best approximates a mineral-associated OC pool
 416 derived from microbially processed plant inputs (Poeplau et al., 2018; Lavallee et al., 2020) and assume that after size
 417 fractionation most of the free organic matter in the bulk soil was in the sand size fraction. We compared the silt+clay size
 418 fraction $\Delta^{14}\text{C}$ values to the bulk $\Delta^{14}\text{C}$ values to determine if the material extracted from the isolated mineral-associated fractions
 419 of the soil had greater OC persistence or if these compounds cycled indiscriminate of mineral association (Fig. 2).

420 While the TLE from the silt+clay and bulk soil had similar $\Delta^{14}\text{C}$ values, the AA from the silt+clay size fraction was
 421 enriched in ^{14}C compared to the AA from bulk soil ($r^2 = 0.98$, $p < 0.05$). This suggests that AAs cycle faster in the silt+clay

422 mineral pool than in the bulk soils. While mineral surfaces usually are thought to promote stability and persistence of OC, in
423 some soil systems, mineral associations may not be the single defining factor of OC persistence (Rocci et al., 2021) and could
424 have a more nuanced role influencing OC cycling in soils.

425 Our data suggests there is a continuum of compounds that exist with different ^{14}C values in the mineral-associated pool,
426 because in the silt+clay fraction, the TLE, AA, and AI have significantly different ^{14}C values (Fig. 4b). For instance, the
427 mineral-associated TLE and AA fractions are enriched in ^{14}C relative to the silt+clay fraction, suggesting both are cycling
428 faster than the average mineral associated pool. However, the AI from the silt+clay fraction is cycling slower than solid sample
429 it was extracted from, and when we compare the AI from the bulk soil to the AI from the silt+clay, the AI from the silt+clay
430 is slightly more ^{14}C enriched. This suggests that there is slight ^{14}C enrichment across compounds in the silt+clay fraction
431 relative to sand and bulk soil.

432 Our data suggests that lipids in mineral-associated OC pools vary in cycling rates. This is complementary to findings from
433 other studies where ^{14}C values from different lipid biomarkers are divergent from the bulk soils (Gies et al., 2021) and indicates
434 the necessity of looking at entire compound class pools for understanding soil carbon persistence. Further investigation into
435 the composition and age-distribution of compounds within mineral associated-OC is needed to better quantify the distribution
436 of cycling rates within mineral associated OC pools.



437

438 **Figure 6: a) $\Delta^{14}\text{C}$ versus soil depth measured for total lipid extractions (TLE) from four soil size/density fractions, the bulk (<2mm),**
439 **sand (63 μm to 2mm), and dense fraction (DF) . b) A comparison of the bulk soil $\Delta^{14}\text{C}$ values to the TLE from the four size/density**
440 **fractions.**

441

442 **4.5 Persistent and Petrogenic OC**

443 The most persistent, oldest OC was found in the AI fraction. Because carbon in the AI cycles more slowly than other
444 components of this grassland soil, it is important to understand what structural components make up the AI and where these
445 compounds are sourced from. Historically, the chemical structure of the AI fraction has been difficult to characterize. Hwang
446 and Druffel (2003) argued that the AI is a lipid-like portion of the ocean OC. However, in soils, the AI can be composed of a
447 mixture of lipid-like compounds and aromatic compounds (Silveira et al., 2008). In our soil, the ^{13}C -NMR spectra of the AI
448 from 0–10 cm depth show a significant, broad peak in the 100–165 ppm range, indicative of aromatics (SI Fig. 3) (Baldock
449 and Preston, 1995; Baldock et al., 1997). While it is possible that some condensed aromatic compounds form during the
450 hydrolysis procedure used to remove AAs, the AI may also contain naturally occurring aromatic compounds that could include
451 pyrogenic or petrogenic OC.

452 The parent material of our site is a mixture of sandstone, shale, greywacke, and schist (Foley et al., 2022), so it is possible
453 that some of the OC in our soils is ancient, rock-derived, petrogenic carbon that has been incorporated into the soil profile
454 through pedogenesis progresses (Grant et al., 2023). Comparison of the AI to the rock (>2 mm) fraction shows that the AI is
455 younger than the OC contained in the rock fraction (SI Table 1), with the rock fraction $\Delta^{14}\text{C}$ values ranging from -481 to -
456 765‰. To calculate the contribution of OC_{petro} into the AI fraction, we used a binary mixing model with endmembers of
457 OC_{petro} and aged SOC based on the method in Grant et al. (2023). The $\Delta^{14}\text{C}$ value of the OC_{petro} ^{14}C endmember is -1000 ‰,
458 which is by definition ^{14}C free, and the $\Delta^{14}\text{C}$ value of the biospheric endmember was set as either the measured TLE $\Delta^{14}\text{C}$
459 value or the bulk $\Delta^{14}\text{C}$ value from each depth. This comparison of these two different biospheric endmembers allowed us to
460 calculate a possible range of values for the OC_{petro} contribution (Table 1). In the AI extracted from the silt+clay fraction, the
461 OC_{petro} contribution was 4–5% from 0–10 cm depth and 40–53 % in the 50–100cm depth. In AI extracted from the bulk soil,
462 the OC_{petro} contribution was 0–1 % in the 0–10 cm depth, and 17–44 % in the 50–100 cm depth. Therefore, while the AI
463 fraction likely contains OC_{petro} , it is primarily composed of OC compounds derived from more recent plant and microbial
464 inputs that are highly resistant to acid hydrolysis either because of their chemical structure or their strong associations with
465 minerals.

466

467 **5 Conclusions and Continued soil radiocarbon compound class characterization**

468 In this study, we characterized a soil carbon profile using compound-class ^{14}C analyses. We found that our extraction
469 methods yielded fractions with ^{14}C signatures distinctly different from the source soil from which they were extracted. We
470 found that in this annual grassland soil, the AA and the TLE fractions cycle more rapidly than the bulk soil throughout the soil
471 profile. At each depth, the AI fraction is the oldest fraction and contains a combination of slowly cycling SOC and ancient
472 petrogenic C. These results show that soil compound classes cycle differently than similar components in marine systems. Our

473 results also show that mineral-associated SOC contains a mixture of carbon compounds with distinctly different ages and
474 sources that drive turnover and persistence. Compound-specific ^{14}C approaches hold promise for improving our understanding
475 of the chemical structure of SOC, as well as the connection between carbon degradation and preservation in soils. A molecule-
476 resolved understanding of the relationship between compound classes and carbon persistence will also give insight into the
477 fate and turnover time of specific organic biomarkers found in plant residues or the biomass of bacteria, fungi and microfauna.
478 These techniques can also help to determine mechanisms promoting mineral stabilization of soil carbon, especially when
479 combined with soil physical fractionation.

480 Results from this study highlight that radiocarbon measurements of specific organic compounds and compound classes in
481 soil provide valuable insights into the persistence and decomposition rates of soil organic carbon. To improve our ability to
482 model the future of soil carbon stocks and soil quality in the face of a changing global climate, we need further research that
483 interrogates the composition, radiocarbon content, and cycling rates of soil organic carbon and mechanistically links these
484 rates to physical and chemical drivers.

485 486 **6 Acknowledgements**

487 This work was performed under the auspices of the U.S. Department of Energy by Lawrence Livermore National Laboratory
488 under Contract DE-AC52-07NA27344 and was supported by the LLNL LDRD Program under Project No. 21-ERD-021 and
489 Project No. 24SI002. LLNL-JRNL-843138. Additional support for site access, sample collection, and site characterization
490 data was provided by the U.S. Department of Energy, Office of Biological and Environmental Research, Genomic Sciences
491 Program LLNL ‘Microbes Persist’ Scientific Focus Area (award #SCW1632). We acknowledge the traditional, ancestral,
492 unceded territory of the Shóqowa and Hopland People, on which this research was conducted. We thank the staff at the Hopland
493 Research and Extension Center who manage the experiment site and Z Kagely for his assistance in digging the soil pit.

494 495 **7 Supplemental Tables/Data Availability**

496 A list of all radiocarbon data, stable carbon, and total OC values with a CAMS tracking number for each of the analyses
497 used in this publication.

498 **8 Author Contributions:** KJM, KMF, TABB, JP, and KEG conceptualized the study. KJM, KMF, TABB, JP secured funding
499 for the project. KEG designed the method and carried out the extractions with input from KJM, KMF, and TABB. CJL carried
500 out the density separations. MNR carried out the water extractions. JDK and MM ran the NMR experiments. KEG, KJM,
501 KMF interpreted the data. KEG prepared the paper with contributions of all co-authors.

502
503 **9 Competing interests.** The authors declare that they have no conflict of interest.

506 **References**

507

508 Agnelli, A., Trumbore, S. E., Corti, G., and Ugolini, F. C.: The dynamics of organic matter in rock fragments in soil
509 investigated by ¹⁴C dating and measurements of ¹³C, *European Journal of Soil Science*, 53, 147-159,
510 <https://doi.org/10.1046/j.1365-2389.2002.00432.x>, 2002.

511 Angst, G., Mueller, K. E., Nierop, K. G. J., and Simpson, M. J.: Plant- or microbial-derived? A review on the molecular
512 composition of stabilized soil organic matter, *Soil Biology and Biochemistry*, 156, 10.1016/j.soilbio.2021.108189, 2021.

513 Angst, G., John, S., Mueller, C. W., Kögel-Knabner, I., and Rethemeyer, J.: Tracing the sources and spatial distribution of
514 organic carbon in subsoils using a multi-biomarker approach, *Scientific Reports*, 6, 1-12, 2016.

515 Bahureksa, W., Tfaily, M. M., Boiteau, R. M., Young, R. B., Logan, M. N., McKenna, A. M., and Borch, T.: Soil Organic
516 Matter Characterization by Fourier Transform Ion Cyclotron Resonance Mass Spectrometry (FTICR MS): A Critical Review
517 of Sample Preparation, Analysis, and Data Interpretation, *Environmental Science & Technology*, 55, 9637-9656,
518 10.1021/acs.est.1c01135, 2021.

519 Baldock, J. A. and Preston, C. M.: Chemistry of Carbon Decomposition Processes in Forests as Revealed by Solid-State
520 Carbon-13 Nuclear Magnetic Resonance, in: *Carbon Forms and Functions in Forest Soils*, 89-117,
521 <https://doi.org/10.2136/1995.carbonforms.c6>, 1995.

522 Baldock, J. A., Oades, J. M., Nelson, P. N., Skene, T. M., Golchin, A., and Clarke, P.: Assessing the extent of decomposition
523 of natural organic materials using solid-state ¹³C NMR spectroscopy, *Soil Research*, 35, 1061-
524 1084, <https://doi.org/10.1071/S97004>, 1997.

525 Bartolome, J. W., James Barry, W., Griggs, T., and Hopkinson, P.: 367Valley Grassland, in: *Terrestrial Vegetation of*
526 *California*, edited by: Barbour, M., University of California Press, 0, 10.1525/california/9780520249554.003.0014, 2007.

527 Blattmann, T. M., Montluçon, D. B., Haghypour, N., Ishikawa, N. F., and Eglinton, T. I.: Liquid Chromatographic Isolation
528 of Individual Amino Acids Extracted From Sediments for Radiocarbon Analysis, *Frontiers in Marine Science*, 7,
529 10.3389/fmars.2020.00174, 2020.

530 Bour, A. L., Walker, B. D., Broek, T. A. B., and McCarthy, M. D.: Radiocarbon Analysis of Individual Amino Acids:
531 Carbon Blank Quantification for a Small-Sample High-Pressure Liquid Chromatography Purification Method, *Analytical*
532 *Chemistry*, 88, 3521-3528, 10.1021/acs.analchem.5b03619, 2016.

533 Broek, T. A. B., Ognibene, T. J., McFarlane, K. J., Moreland, K. C., Brown, T. A., and Bench, G.: Conversion of the
534 LLNL/CAMS 1 MV biomedical AMS system to a semi-automated natural abundance ¹⁴C spectrometer: system
535 optimization and performance evaluation, *Nuclear Instruments and Methods in Physics Research Section B: Beam*
536 *Interactions with Materials and Atoms*, 499, 124-132, 10.1016/j.nimb.2021.01.022, 2021.

537 Buettner, S. W., Kramer, M. G., Chadwick, O. A., and Thompson, A.: Mobilization of colloidal carbon during iron reduction
538 in basaltic soils, *Geoderma*, 221-222, 139-145, <https://doi.org/10.1016/j.geoderma.2014.01.012>, 2014.

539 Coppola, A. I., Wiedemeier, D. B., Galy, V., Haghypour, N., Hanke, U. M., Nascimento, G. S., Usman, M., Blattmann, T.
540 M., Reisser, M., Freymond, C. V., Zhao, M., Voss, B., Wacker, L., Schefuß, E., Peucker-Ehrenbrink, B., Abiven, S.,
541 Schmidt, M. W. I., and Eglinton, T. I.: Global-scale evidence for the refractory nature of riverine black carbon, *Nature*
542 *Geoscience*, 11, 584-588, [10.1038/s41561-018-0159-8](https://doi.org/10.1038/s41561-018-0159-8), 2018.

543 De Troyer, I., Amery, F., Van Moorleghe, C., Smolders, E., and Merckx, R.: Tracing the source and fate of dissolved
544 organic matter in soil after incorporation of a ¹³C labelled residue: A batch incubation study, *Soil Biology and*
545 *Biochemistry*, 43, 513-519, <https://doi.org/10.1016/j.soilbio.2010.11.016>, 2011.

546 Douglas, P. M. J., Pagani, M., Eglinton, T. I., Brenner, M., Curtis, J. H., Breckenridge, A., and Johnston, K.: A long-term
547 decrease in the persistence of soil carbon caused by ancient Maya land use, *Nature Geoscience*, 11, 645-649,
548 [10.1038/s41561-018-0192-7](https://doi.org/10.1038/s41561-018-0192-7), 2018.

549 Dwivedi, D., Riley, W., Torn, M., Spycher, N., Maggi, F., and Tang, J.: Mineral properties, microbes, transport, and plant-
550 input profiles control vertical distribution and age of soil carbon stocks, *Soil Biology and Biochemistry*, 107, 244-259, 2017.

551 Eglinton, T. I., Galy, V. V., Hemingway, J. D., Feng, X., Bao, H., Blattmann, T. M., Dickens, A. F., Gies, H., Giosan, L.,
552 Haghypour, N., Hou, P., Lupker, M., McIntyre, C. P., Montluçon, D. B., Peucker-Ehrenbrink, B., Ponton, C., Schefuss, E.,
553 Schwab, M. S., Voss, B. M., Wacker, L., Wu, Y., and Zhao, M.: Climate control on terrestrial biospheric carbon turnover,
554 *Proc Natl Acad Sci U S A*, 118, [10.1073/pnas.2011585118](https://doi.org/10.1073/pnas.2011585118), 2021.

555 Feng, X., Vonk, J. E., Griffin, C., Zimov, N., Montluçon, D. B., Wacker, L., and Eglinton, T. I.: ¹⁴C Variation of Dissolved
556 Lignin in Arctic River Systems, *ACS Earth and Space Chemistry*, 1, 334-344, [10.1021/acsearthspacechem.7b00055](https://doi.org/10.1021/acsearthspacechem.7b00055), 2017.

557 Feng, X., Benitez-Nelson, B. C., Montluçon, D. B., Prahl, F. G., McNichol, A. P., Xu, L., Repeta, D. J., and Eglinton, T. I.:
558 ¹⁴C and ¹³C characteristics of higher plant biomarkers in Washington margin surface sediments, *Geochimica et*
559 *Cosmochimica Acta*, 105, 14-30, <https://doi.org/10.1016/j.gca.2012.11.034>, 2013.

560 Foley, M. M., Blazewicz, S. J., McFarlane, K. J., Greenlon, A., Hayer, M., Kimbrel, J. A., Koch, B. J., Monsaint-Queeney,
561 V., Morrison, K., Morrissey, E., Hungate, B. A., and Pett-Ridge, J.: Active populations and growth of soil microorganisms
562 are framed by mean annual precipitation in three California annual grasslands, *Soil Biology and Biochemistry*, 108886,
563 <https://doi.org/10.1016/j.soilbio.2022.108886>, 2022.

564 Galy, V., Peucker-Ehrenbrink, B., and Eglinton, T.: Global carbon export from the terrestrial biosphere controlled by
565 erosion, *Nature*, 521, 204-207, [10.1038/nature14400](https://doi.org/10.1038/nature14400), 2015.

566 Galy, V., Beyssac, O., France-Lanord, C., and Eglinton, T.: Recycling of Graphite During Himalayan Erosion: A Geological
567 Stabilization of Carbon in the Crust, *Science*, 322, 943-945, [doi:10.1126/science.1161408](https://doi.org/10.1126/science.1161408), 2008.

568 Gaudinski, J. B., Trumbore, S. E., Davidson, E. A., and Zheng, S.: Soil carbon cycling in a temperate forest: radiocarbon-
569 based estimates of residence times, sequestration rates and partitioning of fluxes, *Biogeochemistry*, 51, 33-69,
570 [10.1023/A:1006301010014](https://doi.org/10.1023/A:1006301010014), 2000.

571 Gies, H., Hagedorn, F., Lupker, M., Montluçon, D., Haghypour, N., van der Voort, T. S., and Eglinton, T. I.: Millennial-age
572 glycerol dialkyl glycerol tetraethers (GDGTs) in forested mineral soils: ¹⁴C-based evidence for stabilization of microbial
573 necromass, *Biogeosciences*, 18, 189-205, [10.5194/bg-18-189-2021](https://doi.org/10.5194/bg-18-189-2021), 2021.

- 574 Gleixner, G.: Soil organic matter dynamics: a biological perspective derived from the use of compound-specific isotopes
575 studies, *Ecological Research*, 28, 683-695, 2013.
- 576 Grant, K. E., Hilton, R. G., and Galy, V. V.: Global patterns of radiocarbon depletion in subsoil linked to rock-derived
577 organic carbon, *Geochemical Perspectives Letters*, 25, 36-40, <https://doi.org/10.7185/geochemlet.2312>, 2023.
- 578 Grant, K. E., Galy, V. V., Haghypour, N., Eglinton, T. I., and Derry, L. A.: Persistence of old soil carbon under changing
579 climate: The role of mineral-organic matter interactions, *Chemical Geology*, 587, 10.1016/j.chemgeo.2021.120629, 2022.
- 580 Hagedorn, F., Saurer, M., and Blaser, P.: A ^{13}C tracer study to identify the origin of dissolved organic carbon in forested
581 mineral soils, *European Journal of Soil Science*, 55, 91-100, <https://doi.org/10.1046/j.1365-2389.2003.00578.x>, 2004.
- 582 Hein, C. J., Usman, M., Eglinton, T. I., Haghypour, N., and Galy, V. V.: Millennial-scale hydroclimate control of tropical
583 soil carbon storage, *Nature*, 581, 63-66, 10.1038/s41586-020-2233-9, 2020.
- 584 Homyak, P. M., Blankinship, J. C., Slessarev, E. W., Schaeffer, S. M., Manzoni, S., and Schimel, J. P.: Effects of altered dry
585 season length and plant inputs on soluble soil carbon, *Ecology*, 99, 2348-2362, <https://doi.org/10.1002/ecy.2473>, 2018.
- 586 Hua, Q., Turnbull, J. C., Santos, G. M., Rakowski, A. Z., Ancapichún, S., De Pol-Holz, R., Hammer, S., Lehman, S. J.,
587 Levin, I., Miller, J. B., Palmer, J. G., and Turney, C. S. M.: ATMOSPHERIC RADIOCARBON FOR THE PERIOD 1950–
588 2019, *Radiocarbon*, 64, 723-745, 10.1017/RDC.2021.95, 2022.
- 589 Huang, Y., Bol, R., Harkness, D. D., Ineson, P., and Eglinton, G.: Post-glacial variations in distributions, ^{13}C and ^{14}C
590 contents of aliphatic hydrocarbons and bulk organic matter in three types of British acid upland soils, *Organic Geochemistry*,
591 24, 273-287, [http://dx.doi.org/10.1016/0146-6380\(96\)00039-3](http://dx.doi.org/10.1016/0146-6380(96)00039-3), 1996.
- 592 Hwang, J. and Druffel, E. R. M.: Lipid-Like Material as the Source of the Uncharacterized Organic Carbon in the Ocean?,
593 *Science*, 299, 881-884, doi:10.1126/science.1078508, 2003.
- 594 Ishikawa, N. F., Itahashi, Y., Blattmann, T. M., Takano, Y., Ogawa, N. O., Yamane, M., Yokoyama, Y., Nagata, T., Yoneda,
595 M., Haghypour, N., Eglinton, T. I., and Ohkouchi, N.: Improved Method for Isolation and Purification of Underivatized
596 Amino Acids for Radiocarbon Analysis, *Analytical Chemistry*, 90, 12035-12041, 10.1021/acs.analchem.8b02693, 2018.
- 597 Jia, J., Liu, Z., Haghypour, N., Wacker, L., Zhang, H., Sierra, C. A., Ma, T., Wang, Y., Chen, L., Luo, A., Wang, Z., He, J.-
598 S., Zhao, M., Eglinton, T. I., and Feng, X.: Molecular ^{14}C evidence for contrasting turnover and temperature sensitivity of
599 soil organic matter components, *Ecology Letters*, 26, 778-788, <https://doi.org/10.1111/ele.14204>, 2023.
- 600 Jobbágy, E. G. and Jackson, R. B.: THE VERTICAL DISTRIBUTION OF SOIL ORGANIC CARBON AND ITS
601 RELATION TO CLIMATE AND VEGETATION, *Ecological Applications*, 10, 423-436, [https://doi.org/10.1890/1051-0761\(2000\)010\[0423:TVDOSO\]2.0.CO;2](https://doi.org/10.1890/1051-0761(2000)010[0423:TVDOSO]2.0.CO;2), 2000.
- 603 Keiluweit, M., Bougoure, J. J., Nico, P. S., Pett-Ridge, J., Weber, P. K., and Kleber, M.: Mineral protection of soil carbon
604 counteracted by root exudates, *Nature Climate Change*, 5, 588-595, 2015.
- 605 Kleber, M., Sollins, P., and Sutton, R.: A conceptual model of organo-mineral interactions in soils: self-assembly of organic
606 molecular fragments into zonal structures on mineral surfaces, *Biogeochemistry*, 85, 9-24, 2007.

- 607 Kleber, M. et al., 2021. Dynamic interactions at the mineral–organic matter interface. *Nature Reviews Earth & Environment*,
608 2(6): 402-421.
- 609 Kögel-Knabner, I.: The macromolecular organic composition of plant and microbial residues as inputs to soil organic matter,
610 *Soil Biology and Biochemistry*, 34, 139-162, [https://doi.org/10.1016/S0038-0717\(01\)00158-4](https://doi.org/10.1016/S0038-0717(01)00158-4), 2002.
- 611 Kotanen, P. M.: Revegetation following Soil Disturbance and Invasion in a Californian Meadow: a 10-year History of
612 Recovery, *Biological Invasions*, 6, 245-254, 10.1023/B:BINV.0000022145.03215.4f, 2004.
- 613 Kuzyakov, Y., Bogomolova, I., and Glaser, B.: Biochar stability in soil: Decomposition during eight years and
614 transformation as assessed by compound-specific ¹⁴C analysis, *Soil Biology and Biochemistry*, 70, 229-236,
615 <http://dx.doi.org/10.1016/j.soilbio.2013.12.021>, 2014.
- 616 Lavallee, J. M., Soong, J. L., and Cotrufo, M. F.: Conceptualizing soil organic matter into particulate and mineral-associated
617 forms to address global change in the 21st century, *Global Change Biology*, 26, 261-273, <https://doi.org/10.1111/gcb.14859>,
618 2020.
- 619 Lechleitner, F. A., Baldini, J. U. L., Breitenbach, S. F. M., Fohlmeister, J., McIntyre, C., Goswami, B., Jamieson, R. A., van
620 der Voort, T. S., Prufer, K., Marwan, N., Culleton, B. J., Kennett, D. J., Asmerom, Y., Polyak, V., and Eglinton, T. I.:
621 Hydrological and climatological controls on radiocarbon concentrations in a tropical stalagmite, *Geochimica et*
622 *Cosmochimica Acta*, 194, 233-252, <https://doi.org/10.1016/j.gca.2016.08.039>, 2016.
- 623 Lehmann, J. and Kleber, M.: The contentious nature of soil organic matter, *Nature*, 528, 60-68, 10.1038/nature16069, 2015.
- 624 Lehmann, J., Hansel, C. M., Kaiser, C., Kleber, M., Maher, K., Manzoni, S., Nunan, N., Reichstein, M., Schimel, J. P., Torn,
625 M. S., Wieder, W. R., and Kögel-Knabner, I.: Persistence of soil organic carbon caused by functional complexity, *Nature*
626 *Geoscience*, 13, 529-534, 10.1038/s41561-020-0612-3, 2020.
- 627 Levin, I., Hesshaimer, V., 2000. Radiocarbon – A Unique Tracer of Global Carbon Cycle Dynamics. *Radiocarbon*, 42(1):
628 69-80.
- 629 Loh, A. N., Bauer, J. E., and Druffel, E. R. M.: Variable ageing and storage of dissolved organic components in the open
630 ocean, *Nature*, 430, 877-881, 10.1038/nature02780, 2004.
- 631 Lützow, M. v., Kögel-Knabner, I., Ekschmitt, K., Matzner, E., Guggenberger, G., Marschner, B., and Flessa, H.:
632 Stabilization of organic matter in temperate soils: mechanisms and their relevance under different soil conditions - a review,
633 *European Journal of Soil Science*, 57, 426-445, 10.1111/j.1365-2389.2006.00809.x, 2006.
- 634 Marin-Spiotta, E., Chadwick, O. A., Kramer, M., and Carbone, M. S.: Carbon delivery to deep mineral horizons in Hawaiian
635 rain forest soils, *Journal of Geophysical Research: Biogeosciences*, 116, 2011.
- 636 McFarlane, K. J., Torn, M. S., Hanson, P. J., Porras, R. C., Swanston, C. W., Callahan, M. A., and Guilderson, T. P.:
637 Comparison of soil organic matter dynamics at five temperate deciduous forests with physical fractionation and radiocarbon
638 measurements, *Biogeochemistry*, 112, 457-476, 10.1007/s10533-012-9740-1, 2013.
- 639 Mikutta, R., Mikutta, C., Kalbitz, K., Scheel, T., Kaiser, K., and Jahn, R.: Biodegradation of forest floor organic matter
640 bound to minerals via different binding mechanisms, *Geochimica et Cosmochimica Acta*, 71, 2569-2590, 2007.

- 641 Moe, L. A.: Amino acids in the rhizosphere: From plants to microbes, *American Journal of Botany*, 100, 1692-1705,
642 <https://doi.org/10.3732/ajb.1300033>, 2013.
- 643 Nuccio, E. E., Anderson-Furgeson, J., Estera, K. Y., Pett-Ridge, J., De Valpine, P., Brodie, E. L., and Firestone, M. K.:
644 Climate and edaphic controllers influence rhizosphere community assembly for a wild annual grass, *Ecology*, 97, 1307-
645 1318, 10.1890/15-0882.1, 2016.
- 646 Poeplau, C., Don, A., Six, J., Kaiser, M., Benbi, D., Chenu, C., Cotrufo, M. F., Derrien, D., Gioacchini, P., Grand, S.,
647 Gregorich, E., Griepentrog, M., Gunina, A., Haddix, M., Kuzyakov, Y., Kühnel, A., Macdonald, L. M., Soong, J., Trigalet,
648 S., Vermeire, M.-L., Rovira, P., van Wesemael, B., Wiesmeier, M., Yeasmin, S., Yevdokimov, I., and Nieder, R.: Isolating
649 organic carbon fractions with varying turnover rates in temperate agricultural soils – A comprehensive method comparison,
650 *Soil Biology and Biochemistry*, 125, 10-26, <https://doi.org/10.1016/j.soilbio.2018.06.025>, 2018.
- 651 Pries, C. E. H., Ryals, R., Zhu, B., Min, K., Cooper, A., Goldsmith, S., Pett-Ridge, J., Torn, M., and Berhe, A. A.: The Deep
652 Soil Organic Carbon Response to Global Change, *Annual Review of Ecology, Evolution, and Systematics*, 54, 375-401,
653 10.1146/annurev-ecolsys-102320-085332, 2023.
- 654 R Core Team: R: A language and environment for statistical computing., R Foundation for Statistical Computing [code],
655 2019.
- 656 Repasch, M., Scheingross, J. S., Hovius, N., Lupker, M., Wittmann, H., Haghypour, N., Gröcke, D. R., Orfeo, O., Eglinton,
657 T. I., and Sachse, D.: Fluvial organic carbon cycling regulated by sediment transit time and mineral protection, *Nature*
658 *Geoscience*, 14, 842-848, 10.1038/s41561-021-00845-7, 2021.
- 659 Rethemeyer, J., Kramer, C., Gleixner, G., Wiesenberger, G. L. B., Schwark, L., Andersen, N., Nadeau, M.-J., and Grootes, P.
660 M.: Complexity of Soil Organic Matter: AMS 14C Analysis of Soil Lipid Fractions and Individual Compounds,
661 *Radiocarbon*, 46, 465-473, 10.1017/S0033822200039771, 2004.
- 662 Rocci, K. S., Lavallee, J. M., Stewart, C. E., and Cotrufo, M. F.: Soil organic carbon response to global environmental
663 change depends on its distribution between mineral-associated and particulate organic matter: A meta-analysis, *Science of*
664 *The Total Environment*, 793, 148569, <https://doi.org/10.1016/j.scitotenv.2021.148569>, 2021.
- 665 Schmidt, M. W., Torn, M. S., Abiven, S., Dittmar, T., Guggenberger, G., Janssens, I. A., Kleber, M., Kögel-Knabner, I.,
666 Lehmann, J., and Manning, D. A.: Persistence of soil organic matter as an ecosystem property, *Nature*, 478, 49-56, 2011.
- 667 Shi, Z., Allison, S. D., He, Y., Levine, P. A., Hoyt, A. M., Beem-Miller, J., Zhu, Q., Wieder, W. R., Trumbore, S., and
668 Randerson, J. T.: The age distribution of global soil carbon inferred from radiocarbon measurements, *Nature Geoscience*, 13,
669 555-559, 2020.
- 670 Sierra, C. A., Müller, M., and Trumbore, S. E.: Modeling radiocarbon dynamics in soils: SoilR version 1.1, *Geoscientific*
671 *Model Development*, 7, 1919-1931, 10.5194/gmd-7-1919-2014, 2014.
- 672 Silveira, M. L., Comerford, N. B., Reddy, K. R., Cooper, W. T., and El-Rifai, H.: Characterization of soil organic carbon
673 pools by acid hydrolysis, *Geoderma*, 144, 405-414, <https://doi.org/10.1016/j.geoderma.2008.01.002>, 2008.
- 674 Smittenberg, R.H., Eglinton, T.I., Schouten, S., Damsté, J.S.S., 2006. Ongoing Buildup of Refractory Organic Carbon in
675 Boreal Soils During the Holocene. *Science*, 314(5803): 1283-1286.

- 676 Stoner, S., Trumbore, S. E., González-Pérez, J. A., Schrumpf, M., Sierra, C. A., Hoyt, A. M., Chadwick, O., and Doetterl, S.:
677 Relating mineral–organic matter stabilization mechanisms to carbon quality and age distributions using ramped thermal
678 analysis, *Philosophical Transactions of the Royal Society A: Mathematical, Physical and Engineering Sciences*, 381,
679 20230139, doi:10.1098/rsta.2023.0139, 2023.
- 680 Stuiver, M. and Polach, H. A.: Discussion Reporting of ¹⁴C Data, *Radiocarbon*, 19, 355-363, 10.1017/s0033822200003672,
681 1977.
- 682 Swain, D. L., Langenbrunner, B., Neelin, J. D., and Hall, A.: Increasing precipitation volatility in twenty-first-century
683 California, *Nature Climate Change*, 8, 427-433, 10.1038/s41558-018-0140-y, 2018.
- 684 Torn, M. S., Swanston, C. W., Castanha, C., and Trumbore, S. E.: Storage and Turnover of Organic Matter in Soil, in:
685 Biophysico-Chemical Processes Involving Natural Nonliving Organic Matter in Environmental Systems, edited by: Senesi,
686 N., Xing, B., and Huang, P. M., Wiley-IUPAC series in biophysico-chemical processes in environmental systems, John Wiley
687 & Sons, Inc., Hoboken, New Jersey, 219-272, 2009.
- 688 Trumbore, S.: Age of Soil Organic Matter and Soil Respiration: Radiocarbon Constraints on Belowground C Dynamics,
689 *Ecological Applications - ECOL APPL*, 10, 399-411, 10.2307/2641102, 2000.
- 690 Trumbore, S. E. and Harden, J. W.: Accumulation and turnover of carbon in organic and mineral soils of the BOREAS
691 northern study area, *Journal of Geophysical Research: Atmospheres*, 102, 28817-28830, 10.1029/97jd02231, 1997.
- 692 Trumbore, S. E. and Zheng, S.: Comparison of Fractionation Methods for Soil Organic Matter ¹⁴C Analysis, *Radiocarbon*,
693 38, 219-229, 10.1017/s0033822200017598, 1996.
- 694 Ukalska-Jaruga, A., Smreczak, B., and Klimkowicz-Pawlas, A.: Soil organic matter composition as a factor affecting the
695 accumulation of polycyclic aromatic hydrocarbons, *Journal of Soils and Sediments*, 19, 1890-1900, 10.1007/s11368-018-
696 2214-x, 2019.
- 697 van der Voort, T. S., Mannu, U., Hagedorn, F., McIntyre, C., Walthert, L., Schleppei, P., Haghypour, N., and Eglinton, T. I.:
698 Dynamics of deep soil carbon – insights from ¹⁴C time series across a climatic gradient, *Biogeosciences*, 16, 3233-3246,
699 10.5194/bg-16-3233-2019, 2019.
- 700 van der Voort, T. S., Zell, C. I., Hagedorn, F., Feng, X., McIntyre, C. P., Haghypour, N., Graf Pannatier, E., and Eglinton, T.
701 I.: Diverse Soil Carbon Dynamics Expressed at the Molecular Level, *Geophysical Research Letters*, 44, 11,840-811,850,
702 10.1002/2017gl076188, 2017.
- 703 Vogel, C., Mueller, C. W., Höschen, C., Buegger, F., Heister, K., Schulz, S., Schloter, M., and Kögel-Knabner, I.:
704 Submicron structures provide preferential spots for carbon and nitrogen sequestration in soils, *Nature Communications*, 5,
705 2014.
- 706 Vogel, J. S., Southon, J. R., Nelson, D. E., and Brown, T. A.: Performance of catalytically condensed carbon for use in
707 accelerator mass spectrometry, *Nuclear Instruments and Methods in Physics Research Section B: Beam Interactions with*
708 *Materials and Atoms*, 5, 289-293, [https://doi.org/10.1016/0168-583X\(84\)90529-9](https://doi.org/10.1016/0168-583X(84)90529-9), 1984.
- 709 von Lutzow, M., Kögel-Knabner, I., Ekschmitt, K., Flessa, H., Guggenberger, G., Matzner, E., and Marschner, B.: SOM
710 fractionation methods: Relevance to functional pools and to stabilization mechanisms, *Soil Biology and Biochemistry*, 39,
711 2183-2207, 2007.

- 712 Wang, X.-C. and Druffel, E. R. M.: Radiocarbon and stable carbon isotope compositions of organic compound classes in
713 sediments from the NE Pacific and Southern Oceans, *Marine Chemistry*, 73, 65-81, [https://doi.org/10.1016/S0304-](https://doi.org/10.1016/S0304-4203(00)00090-6)
714 4203(00)00090-6, 2001.
- 715 Wang, X.-C., Callahan, J., and Chen, R. F.: Variability in radiocarbon ages of biochemical compound classes of high
716 molecular weight dissolved organic matter in estuaries, *Estuarine, Coastal and Shelf Science*, 68, 188-194,
717 [10.1016/j.ecss.2006.01.018](https://doi.org/10.1016/j.ecss.2006.01.018), 2006.
- 718 Wang, X.-C., Druffel, E. R. M., Griffin, S., Lee, C., and Kashgarian, M.: Radiocarbon studies of organic compound classes
719 in plankton and sediment of the northeastern Pacific Ocean, *Geochimica et Cosmochimica Acta*, 62, 1365-1378,
720 [https://doi.org/10.1016/S0016-7037\(98\)00074-X](https://doi.org/10.1016/S0016-7037(98)00074-X), 1998.
- 721
- 722